03.4

Cavitation at the end of an optical fiber during laser heating of water in a narrow slit

© E.P. Dats, A.V. Kulik, M.A. Guzev, V.M. Chudnovskii

Institute for Applied Mathematics, Far East Branch, Russian Academy of Sciences, Vladivostok, Russia
E-mail: datsep@gmail.com

Received April 26, 2023
Revised June 14, 2023
Accepted June 14, 2023

An experimental study of the process of growth and collapse of a cavitation bubble at the tip of an optical fiber placed between flat solid surfaces (in a slot) has been carried out. The features of the dynamics of cavitation bubbles in this configuration are explained using numerical simulation. It is shown that laser cavitation at the tip of an optical fiber can be used for selective cleaning and sanitation of surfaces in slots and channels.

Keywords: lasers, cavitation, numerical simulation.

DOI: 10.61011/TPL.2023.08.56694.19607

Surface cleaning is an important technical problem that is solved efficiently by applying acoustic cavitation [1]. However, selective cleaning of a local small surface area (in particular, in hard-to-reach spots, such as narrow slits and channels) is not feasible in this case. Laser-induced cavitation at the tip of an optical fiber immersed into a liquid is proposed to be used for this purpose. Being highly flexible and capable of penetrating into narrow channels, slits, and puncture needles, optical fiber is a convenient means for transporting laser radiation to various objects. The present study is the first to demonstrate that a collapsing cavitation bubble, which emerges under continuous laser heating of water at the tip of an optical fiber introduced into a narrow slit, provides for efficient selective cleaning of its interior surface.

Laser induced cavitation is observed in the course of liquid boiling at subcooling triggered by either focused laser radiation or radiation emitted from the tip of a radiation-transmitting optical fiber immersed into a liquid. A gas-vapor bubble emerging in the process of boiling at subcooling eventually stops growing due to contact with the surrounding „cool“ liquid and undergoes an accelerated collapse. This dynamics (bubble growth and subsequent collapse) is the actual reason why a bubble is a cavitation one. It is well known that cavitation bubbles near various boundaries generate cumulative jets [2–6] alongside with acoustic signals and shock waves. Taken together, these phenomena have promising practical applications in medicine and selective cleaning and processing of surfaces [7,8]. Within this context, the use of optical fiber for inducing cavitation has certain advantages over other methods (specifically, spark discharge [4] and the technique involving laser radiation focusing [5,8]), but remains understudied.

In what follows, laser induced cavitation at the tip of an optical fiber introduced into a slit filled with water (i.e., a space bounded on two sides by planar metal plates) is examined experimentally and numerically. A semiconductor laser with a wavelength of $1.47\,\mu$m and a power of 5 W was used in experiments. Its radiation was transmitted along quartz-polymer fiber with a quartz core $600\,\mu$m in diameter. Since radiation with a wavelength of $1.47\,\mu$m is absorbed well in water with an absorption coefficient of $\sim 25\,\text{cm}^{-1}$, volumetric liquid boiling may be initiated near the fiber tip. All experiments were carried out in nondeaerated water at a temperature of 22°C in a cuvette $12.5 \times 2.3 \times 4.1$ cm in size with the use of a high-speed PHOTRON FASTCAM SA-Z camera. An elementary boiling event (the dynamics of growth and collapse of a single bubble) was studied. The growth and collapse of a bubble were examined „in transmission“ with light (laser radiation with a wavelength of $\lambda = 520$ nm) propagating through the experimental cuvette in the direction toward the video camera objective. Two aluminum metal plates $10 \times 1 \times 3$ cm in size, which formed the experimental slit, were mounted in the cuvette parallel to each other with a 3 mm gap (slit width) between them. An optical fiber oriented vertically downward was mounted between the plates at a distance of 2 cm from the upper plate boundary and 1.5 cm from the interior plate walls. The distance between the fiber tip and the cuvette bottom was 2 cm.

The problem was solved using the finite volume method in ANSYS Fluent. Calculations were performed by applying the SIMPLE algorithm on a uniform square grid with an element $2\,\mu$m in size. The volume of fluid method [9] with Navier–Stokes equations and the energy balance equation solved for a two-phase liquid/vapor medium was used to approximate the interphase boundary. A one-dimensional problem of determination of the radius of a spherical bubble with its dynamics characterized by the Rayleigh–Plesset equation was solved separately using the finite difference method to find the optimum grid size. The determined motion law for the radius was compared to the result obtained in Fluent without regard to the process of evaporation–condensation and thermal conductivity. It was established

that the difference between the solution obtained in Fluent and the one found by integrating the Rayleigh–Plesset equation was less than 4% at a grid element size of $2\,\mu$m. The maximum difference between the compared solutions at a grid element size of $4\,\mu$m was approximately 12%. A comparison of data calculated with a grid size of $1\,\mu$m and the evaporation-condensation process factored in and the results for a $2\,\mu$m grid size revealed that the laws of motion of the interphase boundary in the process of bubble growth/collapse differ by less than 1%. However, smaller fragments of the vapor phase were observed in the process of repeat boiling on a grid with an element $1\,\mu$m in size; vanishing after repeat condensation, these fragments did not affect the temperature field distribution in the liquid phase. The surface mass exchange between liquid and vapor phases was characterized within the Lee evaporation-condensation model [10], wherein the evaporation-condensation rate is proportional to the difference between the temperature of the medium and the saturation temperature that depends on absolute pressure. The initial conditions of the problem corresponded to parameter estimates derived experimentally.

Figure 1 presents the temporal variation of radius, velocity, and acceleration values for a bubble determined experimentally in a slit. The radius values are measured from the center of the fiber tip axially downward to the interphase boundary.

The values of bubble radius, velocity, and acceleration provide an opportunity to estimate vapor pressure P in a bubble in accordance with the Rayleigh–Plesset equation [11]:

$$P = P_0 + 2\sigma/R(t) + 4\mu\dot{R}(t)/R(t) + \rho_l\left(R(t)\ddot{R}(t) + 1.5\dot{R}^2(t)\right), \qquad (1)$$

where P_0 is the atmospheric pressure, σ is the surface tension coefficient, μ is the dynamic viscosity of water, and ρ_l is the density of water.

Inserting the experimental values (Fig. 1) into (1), one obtains estimates of the pressure and, consequently, the temperature of vapor in a bubble [12]; at the start of the process, $P \approx 6 \cdot 10^5$ Pa and saturation temperature $T \approx 433$ K. These estimates were used as the initial conditions in numerical calculation of the bubble dynamics. The temperature of the liquid medium outside of a bubble was set to be decreasing linearly from 433 to 300 K in a spherical layer $30 < r < 300\,\mu$m in size. A temperature of 300 K was set outside of this layer. Measurements were performed in three experiments. The experimental curve (Fig. 1) was plotted using the mean value. The measurement accuracy is limited by the camera resolution: 1 pixel of the camera image is $20\,\mu$m in size. The apparent width of the interphase boundary is 1 pixel: the gas phase (dark pixels) and the liquid phase (light pixels) are seen clearly in the frames in Fig. 2. A layer 1 pixel in width between these phases belongs to an indeterminate phase. Thus, the error of measurement of the interphase boundary is $20\,\mu$m. Since

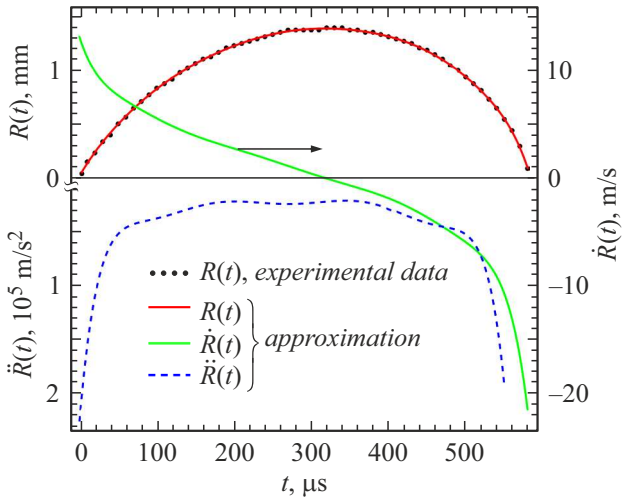

Figure 1. Temporal variation of radius, velocity, and acceleration values for a cavitation bubble observed experimentally.

the apparent bubble diameter at the initial stage of growth falls within the range of 1-2 pixels (from 20 to $40\,\mu$m), a mean value of $30\,\mu$m was used for the initial bubble radius in numerical calculations. A tenth-order polynomial with a time pitch of $20\,\mu$s was used to approximate the radius, velocity, and acceleration of the interphase boundary (Fig. 1) for further use in formula (1). The variance of the initial pressure estimate within the indicated error of measurement of the initial radius ($20 < r < 40\,\mu$m) did not exceed 11%, and the difference between the initial temperature values was below 2%.

The frames in Fig. 2 illustrate the dynamics of a cavitation bubble in a slit. Walls correspond to the left and the right edges of frames. The experimental dynamics of a bubble is presented in a side view. According to the results of numerical calculations reproducing the experimental variation of the bubble radius, regions of excess pressure in the liquid phase form on the walls in the process of bubble growth. Owing to this, the bubble assumes a the shape of a spheroid elongated vertically along the walls (frame 2 in Fig. 2). As the bubble grows further, liquid near the walls gets displaced. Regions with a reduced pressure in the liquid phase form on the walls as a result. This is the reason why the collapsing bubble stretches in the direction normal to the surfaces of walls and assumes the shape of an oblate spheroid (frame 3 in Fig. 2), which then transforms into a dumbbell (frame 4) with the interphase boundary moving toward a reduced pressure. The bubble then disintegrates on the slit walls, producing jets of heated liquid directed normally to the walls (frames 5, 6 in Fig. 2). A heated liquid jet penetrates the space occupied by the vapor phase in this region and, having reached the walls, forms a region of increased excess pressure.

According to the results of numerical calculations, the excess pressure of the liquid phase on the interior slit walls at the moment of collision between the front of a cumulative

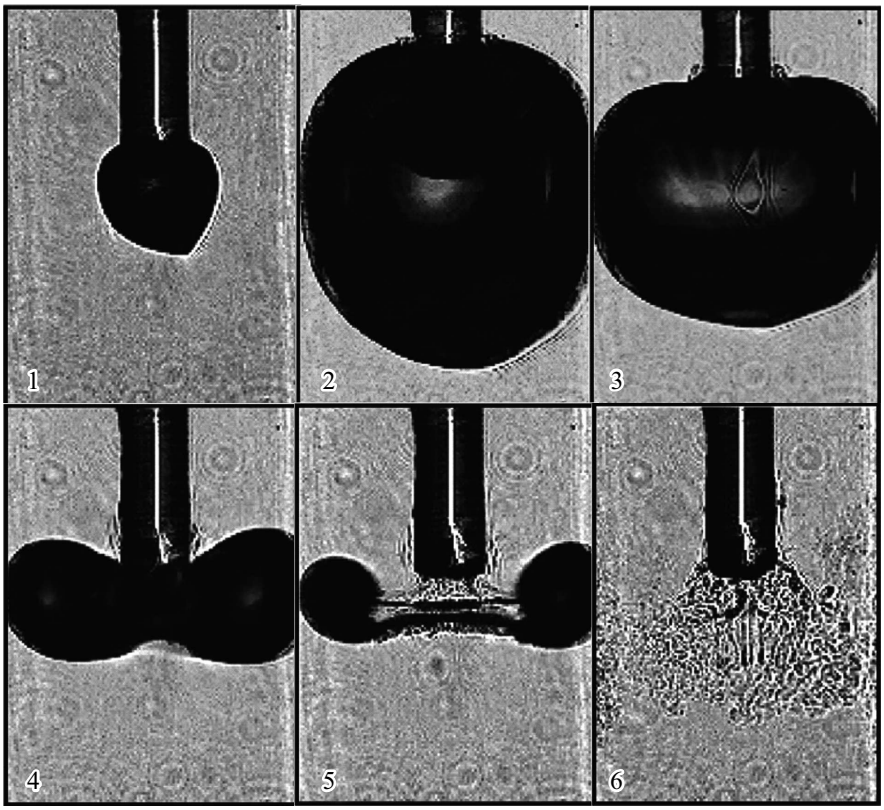

Figure 2. Dynamics of growth and collapse of a vapor bubble in a slit 3000 μm in width filled with nondeaerated water. The fiber diameter is 600 μm. Frames 1–6 correspond to the following intervals of time elapsed from the onset of bubble growth: $t_1 = 80\,\mu$s, $t_2 = 345\,\mu$s, $t_3 = 550\,\mu$s, $t_4 = 560\,\mu$s, $t_5 = 600\,\mu$s, $t_6 = 1000\,\mu$s.

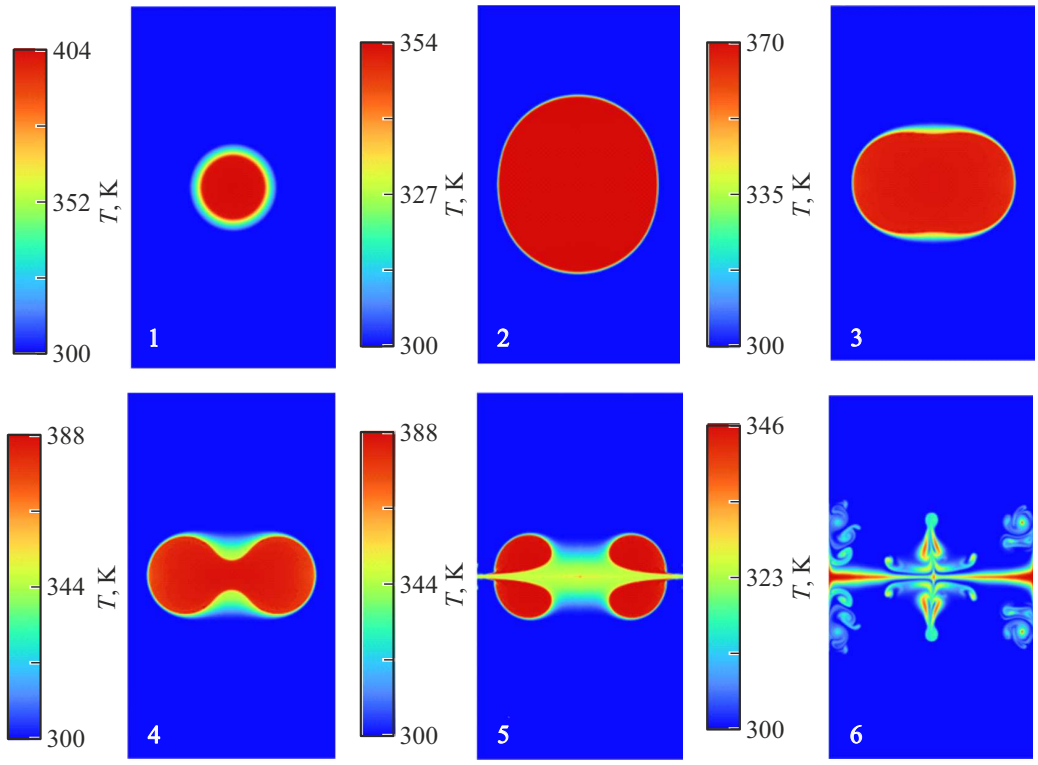

Figure 3. Calculated variation of the temperature field in a two-phase medium in the process of bubble growth-collapse. Frames 1–6 correspond to the following intervals of time elapsed from the onset of bubble growth: $t_1 = 80\,\mu$s, $t_2 = 345\,\mu$s, $t_3 = 550\,\mu$s, $t_4 = 560\,\mu$s, $t_5 = 600\,\mu$s, $t_6 = 1000\,\mu$s.

jet and the surface of plates is as high as 440 kPa, and the jet temperature reaches 343 K (frames 5, 6 in Fig. 3). The obtained estimates of the pressure and temperature in liquid jets produced as a result of laser cavitation in the examined geometry with an optical fiber suggest that this phenomenon may well be used to clean and sanitize the interior walls of a narrow slit.

Funding

This study was supported financially by the Russian Science Foundation (project No. 22-19-00189).

Conflict of interest

The authors declare that they have no conflict of interest.

References

[1] A. Maksimov, J. Acoust. Soc. Am., **151**, 1464 (2022). DOI: 10.1121/10.0009673
[2] V.M. Chudnovskii, V.I. Yusupov, Tech. Phys. Lett., **46**, 1024 (2020). DOI: 10.1134/S1063785020100211.
[3] R.V. Fursenko, V.M. Chudnovskii, S.S. Minaev, J. Okajima, Int. J. Heat Mass Transfer, **163**, 120420 (2020). DOI: 10.1016/j.ijheatmasstransfer.2020.120420 0017-9310
[4] G. Huang, M. Zhang, X. Ma, Q. Chang, C. Zheng, B. Huang, Ultrason. Sonochem., **67**, 105147 (2020). DOI: 10.1016/j.ultsonch.2020.105147
[5] D. Horvat, U. Orthaber, J. Schillec, L. Hartwigc, U. Löschner, A. Vrecko, R. Petkovĕk, Int. J. Multiphase Flow., **100**, 119 (2018). DOI: 10.1016/j.ijmultiphaseflow.2017.12.010
[6] T.P. Adamova, V.M. Chudnovsky, D.S. Elistratov, Tech. Phys. Lett., **48**, 16 (2022). DOI: 10.21883/TPL.2022.01.52459.18991.
[7] D.N. Morenko, V.I. Yusupov, I.A. Abushkin, Yu.P. Pakhalyuk, M.A. Guzev, V.M. Chudnovskii, Flebologiya, **15** (4), 259 (2021) (in Russian). DOI: 10.17116/flebo202115041259
[8] C.-D. Ohl, M. Arora, R. Dijkink, V. Janve, D. Lohse, Appl. Phys. Lett., **89**, 074102 (2006). DOI: 10.1063/1.2337506
[9] C.W. Hirt, B.D. Nichols, J. Comput. Phys., **39**, 201 (1981). DOI: 10.1016/0021-9991(81)90145-5
[10] W.H. Lee, in *Multiphase transport: fundamentals, reactor safety, applications,* ed. by T. Veziroglu (Hemisphere Publ., 1980), vol. 1, p. 407–432.
[11] M. Plesset, A. Prosperetti, Ann. Rev. Fluid Mech., **9**, 145 (1977). DOI: 10.1146/annurev.fl.09.010177.001045
[12] W. Wagner, A. Pruß, J. Phys. Chem. Ref. Data, **31**, 387 (2002). DOI: 10.1063/1.1461829

Translated by D.Safin